

# Supersymmetric cold dark matter with Yukawa unification

M. E. Gómez,<sup>\*</sup> G. Lazarides,<sup>†</sup> and C. Pallis<sup>‡</sup>

Physics Division, School of Technology, Aristotle University of Thessaloniki, Thessaloniki GR 540 06, Greece  
(Received 7 July 1999; published 26 May 2000)

The cosmological relic density of the lightest supersymmetric particle of the minimal supersymmetric standard model is calculated under the assumption of gauge and Yukawa coupling unification. We employ radiative electroweak breaking with universal boundary conditions from gravity-mediated supersymmetry breaking. Coannihilation of the lightest supersymmetric particle, which turns out to be an almost pure  $B$ -ino, with the next-to-lightest supersymmetric particle (the lightest stau) is crucial for reducing its relic density to an acceptable level. Agreement with the mixed or the pure cold (in the presence of a nonzero cosmological constant) dark matter scenarios for large scale structure formation in the universe requires that the lightest stau mass is about 2–8 % larger than the  $B$ -ino mass, which can be as low as 222 GeV. The smallest allowed value of the lightest stau mass turns out to be about 232 GeV.

PACS number(s): 95.35.+d, 12.60.Jv

## I. INTRODUCTION

It is by now clear [1] that in a universe with a zero cosmological constant, a combination of cold plus hot dark matter is needed for fitting the data on cosmic microwave background (CMB) anisotropies and large scale structure [2] in the universe, especially for an essentially flat spectrum of the primordial density fluctuations. The energy density  $\rho$  of the universe is taken equal to its critical value  $\rho_c$  ( $\Omega \equiv \rho/\rho_c = 1$ ), as suggested by inflationary cosmology, and assumed to consist solely of matter ( $\Omega_m = 1$ ). About 10% of matter is baryonic ( $\Omega_B \approx 0.1$ ), while the rest (dark matter) contains a hot component with density equal to about 20% of the critical density ( $\Omega_{\text{HDM}} \approx 0.2$ ) and a cold one with  $\Omega_{\text{CDM}} \approx 0.7$ . The present value of the Hubble parameter in units of  $100 \text{ km sec}^{-1} \text{ Mpc}^{-1}$  is taken to be  $h \approx 0.5$ . Hot dark matter may consist of light neutrinos. This is compatible with atmospheric [3] and solar neutrino oscillations, within a three neutrino scheme, only if light neutrino masses are almost degenerate. A consistent supersymmetric inflationary model with degenerate light neutrino masses providing the hot dark matter in the universe has been constructed in Ref. [4]. Cold dark matter, in the case of a vanishing cosmological constant, must satisfy the relation  $\Omega_{\text{CDM}} h^2 \approx 0.175$ .

Recent observational developments, however, seem to hint towards an alternative picture for the composition of the energy density of the universe with a nonvanishing contribution from something similar to a cosmological constant. Measurements [5] of the cluster baryon fraction combined with the low deuterium abundance constraint [6] on the baryon asymmetry of the universe,  $\Omega_B h^2 \approx 0.02$ , suggest that the matter density is around 35% of the critical density of the universe ( $\Omega_m \approx 0.35$ ). Also, recent observations [7] favor the existence of a cosmological constant, whose contribution to the energy density can be as large as 65% of the critical density ( $\Omega_\Lambda \approx 0.65$ ), driving the total energy density close to its critical value as required by inflation. The as-

sumption that dark matter contains only a cold component leads then to a ‘‘good’’ fit [8] of the CMB radiation and both the large scale structure and age of the universe data. Higher values of the Hubble constant ( $h \approx 0.65$ ) are, however, required and, thus,  $\Omega_{\text{CDM}} \approx 0.3$ . Moreover, the possibility of improving this fit by adding light neutrinos as hot dark matter appears [9] to be rather limited. We can, thus, assume hierarchical neutrino masses in this case. A consistent supersymmetric picture leading ‘‘naturally’’ to hybrid inflation and employing hierarchical neutrino masses has been presented in Ref. [10]. In the presence of a nonvanishing cosmological constant, cold dark matter must satisfy  $\Omega_{\text{CDM}} h^2 \approx 0.125$ .

Both these cosmological models with a zero or nonzero cosmological constant, which provide the best fits to all the available data, are equally plausible alternatives for the composition of the energy density of the universe. Thus, taking into account the observational uncertainties, we will restrict  $\Omega_{\text{CDM}} h^2$  in the range 0.09–0.22.

The lightest supersymmetric particle (LSP) of the minimal supersymmetric standard model (MSSM) is one of the most promising candidates for cold dark matter [11,12]. This is normally the lightest neutralino and its stability is guaranteed by the presence of a discrete  $Z_2$  matter parity, which implies that supersymmetric particles can disappear only by annihilating in pairs. The cosmological relic density of the lightest neutralino can be reliably computed, for various values of the parameters of MSSM, under the assumptions of gauge coupling unification and radiative electroweak breaking with universal boundary conditions from gravity-mediated supersymmetry breaking (see, e.g., Refs. [13–15]). Coannihilation [16] of the LSP with the next-to-lightest supersymmetric particle (NLSP) turns out to be crucial in many cases [13,14,17].

The purpose of this paper is to estimate the lightest neutralino relic density in a specific MSSM framework [18] of the above variety, where the three Yukawa couplings of the third family of quarks and leptons unify ‘‘asymptotically’’ [i.e., at the grand unified theory (GUT) scale  $M_{\text{GUT}} \sim 10^{16} \text{ GeV}$ ]. This can arise by embedding MSSM in a supersymmetric GUT based on a gauge group such as  $\text{SO}(10)$

<sup>\*</sup>Email address: mgomez@cc.uoi.gr

<sup>†</sup>Email address: lazari@eng.auth.gr

<sup>‡</sup>Email address: kpallis@gen.auth.gr

or  $E_6$ , where all the particles of one family belong to a single representation. It is then obvious that requiring the masses of the third family fermions to arise primarily from their unique Yukawa coupling to a particular superfield representation [say a 10-plet of  $SO(10)$ ] predominantly containing the electroweak Higgs bosons guarantees the desired Yukawa coupling unification. This scheme predicts large  $\tan \beta \approx m_t/m_b$ , as well as the successful “asymptotic” mass relation  $m_\tau = m_b$ . The supersymmetric particle spectrum, top quark mass, and Higgs scalar masses in this model have been studied in Refs. [19–21]. The top quark mass is “naturally” restricted to large values compatible with the present experimental data and the supersymmetric particle masses are predicted relatively large. The lightest neutralino is an almost pure  $B$ -ino, whereas the NLSP is the lightest stau mass eigenstate.

Coannihilation of the  $B$ -ino with the NLSP turns out to be of crucial importance for keeping the  $B$ -ino relic density at an acceptably low level. This implies that the lightest stau must not be much heavier than the  $B$ -ino so that coannihilation can be effective. Moreover, increasing the lightest stau to  $B$ -ino mass ratio leads to a larger  $B$ -ino mass which further enhances its relic density. Lightest stau masses of about 2–8 % larger than the  $B$ -ino mass are required for obtaining  $\Omega_{CDM} h^2$  in the range 0.09–0.22. It is interesting to note that, for smaller “relative” mass gaps between the lightest stau and the  $B$ -ino,  $\Omega_{CDM} h^2$  rapidly decreases and becomes unacceptably small. The values of this mass gap which we find here combined with the fact that the  $B$ -ino mass turns out to be greater than about 222 GeV make the lightest stau a phenomenologically interesting charged sparticle with mass which can be as low as  $\approx 232$  GeV. Our analysis provides quite strong restrictions on the sparticle spectrum of MSSM with Yukawa coupling unification.

In Sec. II, the MSSM with Yukawa coupling unification is introduced and its parameters and sparticle spectrum are constrained. In Sec. III, the relic LSP (lightest neutralino) density is calculated by taking into account its coannihilation with the NLSP (lightest stau). In particular, the  $B$ -ino annihilation cross section is estimated in Sec. III A, whereas Sec. III B is devoted to the evaluation of the relevant coannihilation cross sections. Our results on  $\Omega_{LSP} h^2$  are presented and their consequences are discussed in Sec. III C. Finally, our conclusions are summarized in Sec. IV.

## II. MSSM WITH YUKAWA UNIFICATION

We consider the MSSM embedded in some general supersymmetric GUT based on a gauge group such as  $SO(10)$  or  $E_6$  (where all the particles of one family belong to a single representation) with the additional requirement that the top, bottom and tau Yukawa couplings unify [18] at the GUT scale  $M_{GUT}$ . This requirement is easily guaranteed by ensuring that the masses of the third family fermions arise primarily from their unique Yukawa coupling to a single superfield representation which predominantly contains the electroweak Higgs bosons. We further assume that the GUT gauge symmetry breaking occurs in one step. Ignoring the Yukawa cou-

plings of the first and second generation, the effective superpotential below  $M_{GUT}$  is

$$W = \epsilon_{ij}(-h_t H_2 Q_3^j t^c + h_b H_1^i Q_3^j b^c + h_\tau H_1^i L_3^j \tau^c + \mu H_1^i H_2^j), \quad (1)$$

where  $Q_3 = (t, b)$  and  $L_3 = (\nu_\tau, \tau)$  are the quark and lepton  $SU(2)_L$  doublet left handed superfields of the third generation and  $t^c, b^c$  and  $\tau^c$  the corresponding  $SU(2)_L$  singlets. Also,  $H_1, H_2$  are the electroweak Higgs superfields and  $\epsilon_{12} = +1$ . The gravity-mediated soft supersymmetry breaking terms in the scalar potential are given by

$$V_{\text{soft}} = \sum_{a,b} m_{ab}^2 \phi_a^* \phi_b + [\epsilon_{ij}(-A_t h_t H_2^i \tilde{Q}_3^j \tilde{t}^c + A_b h_b H_1^i \tilde{Q}_3^j \tilde{b}^c + A_\tau h_\tau H_1^i \tilde{L}_3^j \tilde{\tau}^c + B \mu H_1^i H_2^j) + \text{H.c.}], \quad (2)$$

where the  $\phi_a$ ’s are the (complex) scalar fields and tildes denote superpartners. The gaugino mass terms in the Lagrangian are

$$\frac{1}{2} \left( M_1 \tilde{B} \tilde{B} + M_2 \sum_{r=1}^3 \tilde{W}_r \tilde{W}_r + M_3 \sum_{a=1}^8 \tilde{g}_a \tilde{g}_a + \text{H.c.} \right), \quad (3)$$

where  $\tilde{B}$ ,  $\tilde{W}_r$ , and  $\tilde{g}_a$  are the  $B$ -ino,  $W$ -inos, and gluinos, respectively. “Asymptotic” Yukawa coupling unification implies

$$h_t(M_{GUT}) = h_b(M_{GUT}) = h_\tau(M_{GUT}) \equiv h_0. \quad (4)$$

Based on  $N=1$  supergravity, we take universal soft supersymmetry breaking terms at  $M_{GUT}$ , i.e., a common mass for the scalar fields  $m_0$ , a common trilinear scalar coupling  $A_0$ , and  $B_0 = A_0 - m_0$ . Also, a common gaugino mass  $M_{1/2}$  is assumed at  $M_{GUT}$ .

Our effective theory below  $M_{GUT}$  depends on the parameters  $[\mu_0 = \mu(M_{GUT})]$

$$m_0, M_{1/2}, A_0, \mu_0, \alpha_G, M_{GUT}, h_0, \tan \beta.$$

The quantities  $\alpha_G = g_G^2/4\pi$  ( $g_G$  being the GUT gauge coupling constant) and  $M_{GUT}$  are evaluated consistently with the experimental values of  $\alpha_{\text{em}}$ ,  $\alpha_s$ , and  $\sin^2 \theta_W$  at  $m_Z$ . We integrate numerically the renormalization group equations (RGEs) for the MSSM at two loops in the gauge and Yukawa couplings from  $M_{GUT}$  down to a common supersymmetry threshold  $M_S \sim 1$  TeV. From this energy to  $m_Z$ , the RGEs of the nonsupersymmetric standard model are used. The set of RGEs needed for our computation can be found in many references (see, for example, Ref. [22]). We take  $\alpha_s(m_Z) = 0.12 \pm 0.001$  which, as it turns out, leads to gauge coupling unification at  $M_{GUT}$  with an accuracy better than 0.1 %. This allows us to assume an exact unification once the appropriate supersymmetric particle thresholds are taken into account. Our integration procedure relies on iterative runs of the RGEs from  $M_{GUT}$  to low energies and back, for every set of values of the input parameters, until agreement with the experimental data is achieved. The value of  $\tan \beta$  at  $M_S$  is estimated using the experimental input

$m_\tau(m_\tau) = 1.777$  GeV and  $M_S$  is fixed to be 1 TeV throughout our calculation. Assuming radiative electroweak symmetry breaking, we can express the values of the parameters  $\mu$  (up to its sign) and  $B$  at  $M_S$  in terms of the other input parameters by means of the appropriate conditions

$$\begin{aligned} \mu^2 &= \frac{m_{H_1}^2 - m_{H_2}^2 \tan^2 \beta}{\tan^2 \beta - 1} - \frac{1}{2} m_Z^2, \\ \sin 2\beta &= -\frac{2B\mu}{m_{H_1}^2 + m_{H_2}^2 + 2\mu^2}, \end{aligned} \quad (5)$$

where  $m_{H_1}, m_{H_2}$  are the soft supersymmetry breaking Higgs boson masses. Here, following Ref. [23], we used the tree-level renormalization group improved scalar potential minimized at a scale comparable to the mass of the top squark. This is adequate for our purposes since, as we find, the corrections to  $\mu$  from the full one-loop effective potential in Ref. [24] are negligible. The sign of  $\mu$  is taken to

be negative (with our conventions), which leads to acceptable predictions for  $b \rightarrow s \gamma$  in models with large  $\tan \beta$  [25].

The common value of the third generation Yukawa coupling at  $M_{\text{GUT}}$  is found by fixing the top quark mass at the center of its experimental range,  $m_t(m_t) = 166$  GeV. The value obtained for  $m_b(m_Z)$  after including supersymmetric corrections is somewhat higher than the experimental limit [26]. We are left with  $m_0$ ,  $M_{1/2}$ , and  $A_0$  as free input parameters. Our results, as it turns out, depend very little on the exact value of  $A_0$  which is, thus, fixed to zero in our calculation. The values of  $m_0$  and  $M_{1/2}$  are found as functions of the tree-level mass  $m_A$  of the  $CP$ -odd Higgs boson  $A$ , for each “relative” mass splitting between the NLSP (lightest stau) and the LSP (almost a pure  $B$ -ino), as we will explain later. The value of  $m_A$  is evaluated at  $M_S$  which is comparable with  $\sqrt{m_t m_{\tilde{t}}}$  [27]. Although the full one-loop corrections to  $m_A$  (from Ref. [24]) are not totally negligible, we will ignore them here since their effect on the LSP relic density is small.

The LSP is the lightest neutralino  $\tilde{\chi}$ . The mass matrix for the four neutralinos is

$$\begin{pmatrix} M_1 & 0 & -m_Z s_W \cos \beta & m_Z s_W \sin \beta \\ 0 & M_2 & m_Z c_W \cos \beta & -m_Z c_W \sin \beta \\ -m_Z s_W \cos \beta & m_Z c_W \cos \beta & 0 & \mu \\ m_Z s_W \sin \beta & -m_Z c_W \sin \beta & \mu & 0 \end{pmatrix}, \quad (6)$$

in the  $(-i\tilde{B}, -i\tilde{W}_3, \tilde{H}_1, \tilde{H}_2)$  basis. Here  $s_W = \sin \theta_W$ ,  $c_W = \cos \theta_W$ , and  $M_1, M_2$  are the mass parameters of  $\tilde{B}, \tilde{W}_3$  in Eq. (3). For the values of  $\mu$  obtained from the radiative electroweak breaking conditions here ( $\mu/M_{1/2} \approx 1.2$ ), the lightest neutralino turns out to be a  $B$ -ino  $\tilde{B}$  with purity  $> 98\%$ .

Large  $b$  and  $\tau$  Yukawa couplings cause soft supersymmetry breaking masses of the third generation squarks and sleptons to run (at low energies) to lower physical values than

the corresponding masses of the first and second generation. Furthermore, the large values of  $\tan \beta$  implied by the unification of the third generation Yukawa couplings lead to large off-diagonal mixings in the sbottom and stau mass-squared matrices. These effects make the physical mass of the lightest stau significantly lower than the masses of the other squarks and sleptons (see below). The NLSP is, thus, the lightest stau mass eigenstate  $\tilde{\tau}_2$  and its mass is obtained by diagonalizing the stau mass-squared matrix

$$\begin{pmatrix} m_\tau^2 + m_{\tilde{\tau}_L}^2 + m_Z^2(-1/2 + s_W^2) \cos 2\beta & m_\tau(A_\tau + \mu \tan \beta) \\ m_\tau(A_\tau + \mu \tan \beta) & m_\tau^2 + m_{\tilde{\tau}_R}^2 - m_Z^2 s_W^2 \cos 2\beta \end{pmatrix}, \quad (7)$$

in the gauge basis  $(\tilde{\tau}_L, \tilde{\tau}_R)$ . Here,  $m_{\tilde{\tau}_{L(R)}}$  is the soft supersymmetry breaking mass of  $\tilde{\tau}_{L(R)}$  and  $m_\tau$  the tau lepton mass. The stau mass eigenstates are

$$\begin{pmatrix} \tilde{\tau}_1 \\ \tilde{\tau}_2 \end{pmatrix} = \begin{pmatrix} c_\theta & s_\theta \\ -s_\theta & c_\theta \end{pmatrix} \begin{pmatrix} \tilde{\tau}_L \\ \tilde{\tau}_R \end{pmatrix}, \quad (8)$$

where  $s_\theta = \sin \theta$ ,  $c_\theta = \cos \theta$ , with  $\theta$  being the  $\tilde{\tau}_L - \tilde{\tau}_R$  mixing angle. Another effect of the large values of the  $b$  and  $\tau$  Yukawa couplings is the reduction of the mass of the  $CP$ -odd Higgs boson  $m_A$  and, consequently, the other Higgs boson masses to smaller values.

The authors of Ref. [21] found that, for every value of  $m_A$  and a fixed value of  $m_t(m_t)$ , there is a pair of minimal values

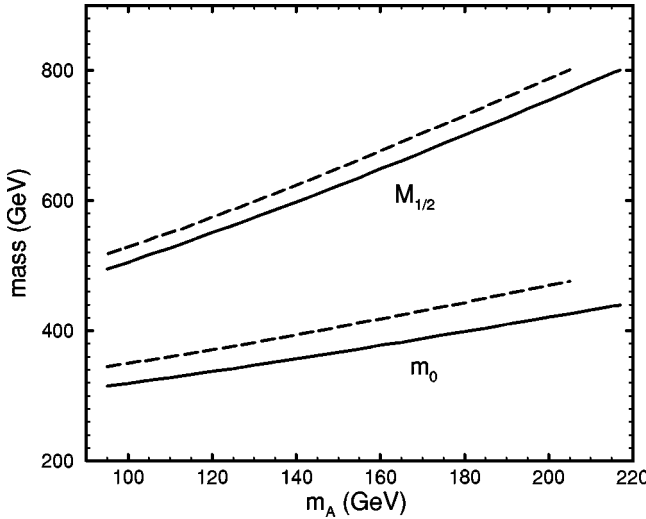


FIG. 1. The mass parameters  $m_0$  and  $M_{1/2}$  as functions of  $m_A$  for  $\Delta_{\tilde{\tau}_2}=0.02$  (solid lines) and  $0.08$  (dashed lines).

of  $m_0$  and  $M_{1/2}$  where the masses of the LSP and  $\tilde{\tau}_2$  are equal. This is understood from the dependence of  $m_A$  on  $m_0$  and  $M_{1/2}$  given in Ref. [20]:

$$m_A^2 = \alpha M_{1/2}^2 - \beta m_0^2 - \text{const}, \quad (9)$$

where all the coefficients are positive and  $\alpha$  and  $\beta$ , which depend only on  $m_t(m_t)$ , are  $\sim 0.1$  (the constant turns out to be numerically close to  $m_Z^2$ ). Equating the masses of the LSP and  $\tilde{\tau}_2$  is equivalent to relating  $m_0$  and  $M_{1/2}$ . Then, for every  $m_A$ , a pair of values of  $m_0$  and  $M_{1/2}$  is determined. Note that Eq. (9) implies the existence of an upper bound on  $m_A$  since  $m_A^2 < \alpha M_{1/2}^2$ . We set here an upper limit on  $M_{1/2}$  equal to 800 GeV, which keeps the sparticle masses below about 2 TeV consistently with our choice for  $M_S$  ( $= 1$  TeV). This limit constrains  $m_A$  to be smaller than  $\approx 220$  GeV. On the other hand, the experimental searches for the lightest  $CP$ -even neutral Higgs boson  $h$  with mass  $m_h$  set a lower limit on  $m_A$ . Taking into account radiative corrections [28,29] in calculating  $m_h$ , we found that this lower limit on  $m_A$  is about 95 GeV. The highest values of  $m_h$ , which are obtained as  $m_A$  increases to its upper limit, lie between 125 and 130 GeV.

Following the procedure of Ref. [21], one can determine  $m_0$  and  $M_{1/2}$  not only for equal masses of the LSP and NLSP but for any relation between these masses. We fix  $m_t(m_t) = 166$  GeV ( $\tan \beta \approx 52.9$ ). For every  $m_A$  and a given ‘‘relative’’ mass splitting  $\Delta_{\tilde{\tau}_2} = (m_{\tilde{\tau}_2} - m_{\tilde{\chi}})/m_{\tilde{\chi}}$  between the NLSP and LSP, we find  $m_0$  and  $M_{1/2}$ . They are depicted in Fig. 1 as functions of  $m_A$  for  $\Delta_{\tilde{\tau}_2} = 0.02$  and  $0.08$  (see Sec. III C). We observe that, for fixed  $m_A$ ,  $M_{1/2}$  increases with  $\Delta_{\tilde{\tau}_2}$ . Thus,  $m_0$  and the sparticle masses increase too with  $\Delta_{\tilde{\tau}_2}$  [see Eq. (9)]. Also, for fixed  $M_{1/2}$ ,  $m_A$  is a decreasing function of  $\Delta_{\tilde{\tau}_2}$ . As a consequence, the upper bound on  $m_A$  (corresponding to  $M_{1/2} = 800$  GeV) gets reduced as  $\Delta_{\tilde{\tau}_2}$  increases. This is why the curves in Fig. 1 which correspond to higher  $\Delta_{\tilde{\tau}_2}$ ’s

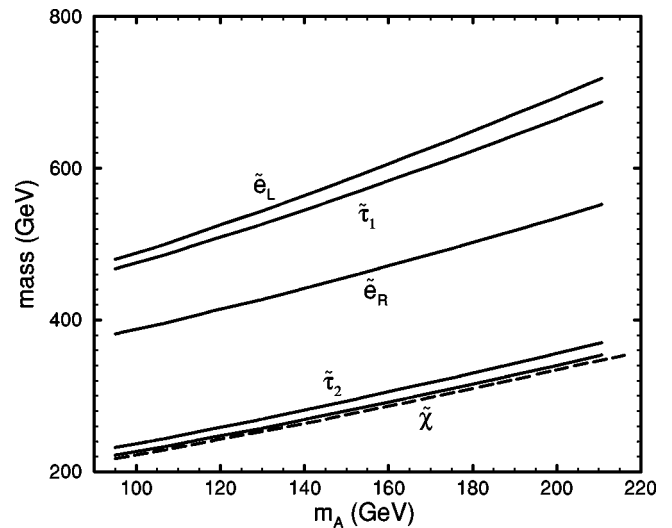


FIG. 2. The relevant part of the sparticle spectrum as a function of  $m_A$  for  $\Delta_{\tilde{\tau}_2}=0.047$ . The LSP mass, for  $\Delta_{\tilde{\tau}_2}=0.02$ , is also included (dashed line).

terminate at smaller  $m_A$ ’s. As we will see, the cosmological bounds on  $\Omega_{\text{LSP}} h^2$  will constrain  $\Delta_{\tilde{\tau}_2}$ . The relevant part of the sparticle spectrum as a function of  $m_A$ , for  $\Delta_{\tilde{\tau}_2}=0.047$ , is shown in Fig. 2. The LSP mass, for  $\Delta_{\tilde{\tau}_2}=0.02$ , is also included.

### III. LSP RELIC DENSITY

We now turn to the calculation of the cosmological relic density of the lightest neutralino  $\tilde{\chi}$  (almost pure  $\tilde{B}$ ) in MSSM with Yukawa unification. As mentioned in Sec. I,  $\Omega_{\tilde{\chi}} h^2$  increases to unacceptably high values as  $m_{\tilde{\chi}}$  becomes larger. Low values of  $m_{\tilde{\chi}}$  are obtained when the NLSP ( $\tilde{\tau}_2$ ) is almost degenerate with  $\tilde{\chi}$ . Under these circumstances, coannihilation of  $\tilde{\chi}$  with  $\tilde{\tau}_2$  and  $\tilde{\tau}_2^*$  is of crucial importance reducing further the  $\tilde{\chi}$  relic density by a significant amount. The important role of coannihilation of the LSP with sparticles carrying masses close to its mass in the calculation of the LSP relic density has been pointed out by many authors (see, e.g., Refs. [13,14,16]). Here, we will use the method described by Griest and Seckel [16]. Note that our analysis can be readily applied to any MSSM scheme where the LSP and NLSP are the  $B$ -ino and stau, respectively.

The relevant quantity, in our case, is the total number density

$$n = n_{\tilde{\chi}} + n_{\tilde{\tau}_2} + n_{\tilde{\tau}_2^*}, \quad (10)$$

since the  $\tilde{\tau}_2$ ’s and  $\tilde{\tau}_2^*$ ’s decay into  $\tilde{\chi}$ ’s after freeze-out. At cosmic temperatures relevant for freeze-out, the scattering rates of these (nonrelativistic) sparticles off particles in the thermal bath are much faster than their annihilation rates since the (relativistic) particles in the bath are considerably more abundant. Consequently, the number densities  $n_i$  ( $i = \tilde{\chi}, \tilde{\tau}_2, \tilde{\tau}_2^*$ ) are proportional to their equilibrium values  $n_i^{eq}$

TABLE I. Feynman diagrams.

Initial state	Final state	Diagrams
$\tilde{\chi}\tilde{\chi}$	$\tau\bar{\tau}$	$t(\tilde{\tau}_{1,2}), u(\tilde{\tau}_{1,2})$
	$e\bar{e}$	$t(\tilde{e}_R), u(\tilde{e}_R)$
$\tilde{\chi}\tilde{\tau}_2$	$th, \tau H, \tau Z$	$s(\tau), t(\tilde{\tau}_{1,2})$
	$\tau A$	$s(\tau), t(\tilde{\tau}_1)$
	$\tau\gamma$	$s(\tau), t(\tilde{\tau}_2)$
$\tilde{\tau}_2\tilde{\tau}_2$	$\tau\tau$	$t(\tilde{\chi}), u(\tilde{\chi})$
$\tilde{\tau}_2\tilde{\tau}_2^*$	$hh, hH, HH, ZZ$	$s(h), s(H), t(\tilde{\tau}_{1,2}), u(\tilde{\tau}_{1,2}), c$
	$AA$	$s(h), s(H), t(\tilde{\tau}_1), u(\tilde{\tau}_1), c$
	$H^+H^-, W^+W^-$	$s(h), s(H), s(\gamma), s(Z), c$
	$\gamma\gamma, \gamma Z$	$t(\tilde{\tau}_2), u(\tilde{\tau}_2), c$
	$t\bar{t}, b\bar{b}$	$s(h), s(H), s(\gamma), s(Z)$
	$\tau\bar{\tau}$	$s(h), s(H), s(\gamma), s(Z), t(\tilde{\chi})$
	$u\bar{u}, d\bar{d}, e\bar{e}$	$s(\gamma), s(Z)$

to a good approximation, i.e.,  $n_i/n \approx n_i^{eq}/n^{eq} \equiv r_i$ . The Boltzmann equation (see e.g., Ref. [30]) is then written as

$$\frac{dn}{dt} = -3Hn - \langle \sigma_{\text{eff}} v \rangle (n^2 - (n^{eq})^2), \quad (11)$$

where  $H$  is the Hubble parameter,  $v$  is the “relative velocity” of the annihilating particles,  $\langle \dots \rangle$  denotes thermal averaging, and  $\sigma_{\text{eff}}$  is the effective cross section defined by

$$\sigma_{\text{eff}} = \sum_{i,j} \sigma_{ij} r_i r_j, \quad (12)$$

with  $\sigma_{ij}$  being the total cross section for particle  $i$  to annihilate with particle  $j$  averaged over initial spin and particle-antiparticle states. In our case,  $\sigma_{\text{eff}}$  takes the form

$$\sigma_{\text{eff}} = \sigma_{\tilde{\chi}\tilde{\chi}} r_{\tilde{\chi}} r_{\tilde{\chi}} + 4\sigma_{\tilde{\chi}\tilde{\tau}_2} r_{\tilde{\chi}} r_{\tilde{\tau}_2} + 2(\sigma_{\tilde{\tau}_2\tilde{\tau}_2} + \sigma_{\tilde{\tau}_2\tilde{\tau}_2^*}) r_{\tilde{\tau}_2} r_{\tilde{\tau}_2}. \quad (13)$$

For  $r_i$ , we use the nonrelativistic approximation

$$r_i(x) = \frac{g_i(1 + \Delta_i)^{3/2} e^{-\Delta_i x}}{g_{\text{eff}}}, \quad (14)$$

$$g_{\text{eff}}(x) = \sum_i g_i(1 + \Delta_i)^{3/2} e^{-\Delta_i x},$$

$$\Delta_i = (m_i - m_{\tilde{\chi}})/m_{\tilde{\chi}}. \quad (15)$$

Here  $g_i = 2, 1, 1$  ( $i = \tilde{\chi}, \tilde{\tau}_2, \tilde{\tau}_2^*$ ) is the number of degrees of freedom of the particle species  $i$  with mass  $m_i$  and  $x = m_{\tilde{\chi}}/T$  with  $T$  being the photon temperature.

In Table I, we list all the Feynman graphs included in the calculation of the effective cross section. The exchanged particles are indicated for each relevant pair of initial and final states. The symbols  $s(x)$ ,  $t(x)$  and  $u(x)$  denote tree-graphs in which the particle  $x$  is exchanged in the  $s$ ,  $t$ , or  $u$  channel. The symbol  $c$  stands for “contact” diagrams with all four

external legs meeting at a vertex.  $H$  and  $H^\pm$  denote the heaviest neutral and the charged Higgs bosons, while  $e$ ,  $\tilde{e}_R$ ,  $u$ , and  $d$  represent the first and second generation charged leptons, charged right handed sleptons, up- and down-type quarks. The other possible reactions  $\tilde{\tau}_2\tilde{\tau}_2^* \rightarrow h[H]A$ ,  $h[H]\gamma$ ,  $h[H]Z$ ,  $AZ$ ,  $H^-W^+$  or  $\nu\bar{\nu}$  ( $\nu$  stands for all three neutrinos) have not been included since they are utterly suppressed by small couplings and/or heavy masses. Also, the tiny contributions from graphs with  $h$  and  $H$  exchange in the  $s$  channel, in the cases of  $u\bar{u}$ ,  $d\bar{d}$ ,  $e\bar{e}$  final states, are left out. Some of the graphs listed here have not been considered in previous works [14] with small  $\tan\beta$ .

The relic abundance of the LSP at the present cosmic time can be calculated from the equation [16,30]

$$\Omega_{\tilde{\chi}} h^2 \approx \frac{1.07 \times 10^9 \text{ GeV}^{-1}}{g_*^{1/2} M_P x_F^{-1} \hat{\sigma}_{\text{eff}}} \quad (16)$$

with

$$\hat{\sigma}_{\text{eff}} \equiv x_F \int_{x_F}^{\infty} \langle \sigma_{\text{eff}} v \rangle x^{-2} dx. \quad (17)$$

Here  $M_P = 1.22 \times 10^{19}$  GeV is the Planck scale,  $g_* \approx 81$  is the effective number of massless degrees of freedom at freeze-out [30], and  $x_F = m_{\tilde{\chi}}/T_F$ , with  $T_F$  being the freeze-out photon temperature calculated by solving iteratively the equation [30,31]

$$x_F = \ln \frac{0.038 g_{\text{eff}}(x_F) M_P (c+2) c m_{\tilde{\chi}} \langle \sigma_{\text{eff}} v \rangle (x_F)}{g_*^{1/2} x_F^{1/2}}. \quad (18)$$

The constant  $c$  is chosen to be equal to 1/2 [31]. The freeze-out temperatures which we obtain here are of the order of  $m_{\tilde{\chi}}/25$  and, thus, our nonrelativistic approximation [see Eq. (14)] is justified. Under these circumstances, the quantities  $\sigma_{ij}v$  are well approximated by their Taylor expansion up to second order in the “relative velocity,”

$$\sigma_{ij}v = a_{ij} + b_{ij}v^2. \quad (19)$$

The thermally averaged cross sections are then easily calculated

$$\langle \sigma_{ij}v \rangle (x) = \frac{x^{3/2}}{2\sqrt{\pi}} \int_0^{\infty} dv v^2 (\sigma_{ij}v) e^{-xv^2/4} = a_{ij} + 6b_{ij}/x. \quad (20)$$

Using Eqs. (12), (13), (17), and (20), one obtains

$$\hat{\sigma}_{\text{eff}} = \sum_{(ij)} (\alpha_{(ij)} a_{ij} + \beta_{(ij)} b_{ij}) \equiv \sum_{(ij)} \hat{\sigma}_{(ij)}, \quad (21)$$

where we sum over  $(ij) = (\tilde{\chi}\tilde{\chi}), (\tilde{\chi}\tilde{\tau}_2)$ , and  $(\tilde{\tau}_2\tilde{\tau}_2^*)$  with  $a_{\tilde{\tau}_2\tilde{\tau}_2^*} = a_{\tilde{\tau}_2\tilde{\tau}_2} + a_{\tilde{\tau}_2\tilde{\tau}_2^*}$ ,  $b_{\tilde{\tau}_2\tilde{\tau}_2^*} = b_{\tilde{\tau}_2\tilde{\tau}_2} + b_{\tilde{\tau}_2\tilde{\tau}_2^*}$ , and  $\alpha_{(ij)}, \beta_{(ij)}$  given by

$$\alpha_{(ij)} = c_{(ij)} x_F \int_{x_F x}^{\infty} \frac{dx}{x^2} r_i(x) r_j(x),$$

$$\beta_{(ij)} = 6 c_{(ij)} x_F \int_{x_F x}^{\infty} \frac{dx}{x^3} r_i(x) r_j(x). \quad (22)$$

Here  $c_{(ij)} = 1, 4, 2$  for  $(ij) = (\tilde{\chi}\tilde{\chi}), (\tilde{\chi}\tilde{\tau}_2)$  and  $(\tilde{\tau}_2\tilde{\tau}_2^{(*)})$ . For  $\Delta_{\tilde{\tau}_2} = 0, \alpha_{(ij)} = 1/4, 1/2, 1/8$  for  $(ij) = (\tilde{\chi}\tilde{\chi}), (\tilde{\chi}\tilde{\tau}_2), (\tilde{\tau}_2\tilde{\tau}_2^{(*)})$ , while  $\beta_{(ij)} = 3\alpha_{(ij)}/x_F$ .

### A. Annihilation cross section

The fact that the LSP ( $\tilde{\chi}$ ) is an almost pure  $\tilde{B}$  implies that the main contribution to its annihilation cross section arises from sfermion (squark, slepton) exchange in the  $t$  and  $u$  channel leading to  $f\bar{f}$  final states ( $f$  is a quark or lepton). The  $s$  channel diagrams are suppressed since the values of  $m_{\tilde{\chi}}$  obtained here are always far from  $m_Z/2$  and  $m_h/2$  (see e.g., Ref. [13]). Moreover, diagrams with quarks in the final state are suppressed relative to the ones with leptons because of the heavier masses of the exchanged squarks and the smaller quark hypercharges. As mentioned in Sec. II, under the assumption of unification of the third family Yukawa couplings,  $m_{\tilde{\tau}_2}$  is smaller than the masses of the other sleptons, hence the production of  $\tau\bar{\tau}$  is enhanced relative to the production of lighter leptons.

Using the partial wave expansion of Ref. [13] and neglecting the masses of the final state leptons, we evaluate the coefficients  $a_{\tilde{\chi}\tilde{\chi}}$  and  $b_{\tilde{\chi}\tilde{\chi}}$  in Eq.(19). They are found to be

$$a_{\tilde{\chi}\tilde{\chi}} = \frac{e^4}{2\pi c_W^4} s_\theta^2 c_\theta^2 Y_L^2 Y_R^2 m_{\tilde{\chi}}^2 \left( \frac{1}{\Sigma_2} - \frac{1}{\Sigma_1} \right)^2, \quad (23)$$

$$b_{\tilde{\chi}\tilde{\chi}} = \frac{e^4}{12\pi c_W^4} \frac{m_{\tilde{\chi}}^2}{\Sigma_2^4} \left[ (s_\theta^4 Y_L^4 + c_\theta^4 Y_R^4) (m_{\tilde{\chi}}^4 + m_{\tilde{\tau}_2}^4) \right. \\ \left. + \frac{s_\theta^2 c_\theta^2 Y_L^2 Y_R^2}{2} (m_{\tilde{\chi}}^4 + 9m_{\tilde{\tau}_2}^4 - 2m_{\tilde{\chi}}^2 m_{\tilde{\tau}_2}^2) \right] \\ + \frac{e^4}{12\pi c_W^4} \frac{m_{\tilde{\chi}}^2 (m_{\tilde{\chi}}^4 + m_{\tilde{e}_R}^4)}{\Sigma_e^4}, \quad (24)$$

where  $Y_{L(R)} = -1/2(-1)$  is the hypercharge of  $\tau_{L(R)}$ ,  $\Sigma_{1,2} = m_{\tilde{\chi}}^2 + m_{\tilde{\tau}_{1,2}}^2$ , and  $\Sigma_e = m_{\tilde{\chi}}^2 + m_{\tilde{e}_R}^2$  with  $m_{\tilde{e}_R}$  being the common (see below) mass of the right handed sleptons  $\tilde{e}_R, \tilde{\mu}_R$  of the two lighter families. Some comments are now in order.

(i) The presence of a nonvanishing coefficient  $a_{\tilde{\chi}\tilde{\chi}}$  is due to the large values of  $\tan\beta$  which lead to an enhancement of the off-diagonal terms in the stau mass-squared matrix in Eq. (7). Indeed, this coefficient is negligible in the case of small  $\tilde{\tau}_L\tilde{\tau}_R$  mixing (i.e., for low  $\tan\beta$ ) where the  $\tilde{\tau}_2$  essentially coincides with  $\tilde{\tau}_R$ . This is due to the fact that the  $s$ -wave contribution, which is the only contribution to  $a_{\tilde{\chi}\tilde{\chi}}$ , is suppressed by factors of the final state fermion mass as one can

show by employing Fermi statistics arguments [11]. For large  $\tan\beta$ , however, this suppression is not complete and  $a_{\tilde{\chi}\tilde{\chi}}$  is proportional to  $\sin^2\theta$ . Despite the fact that  $a_{\tilde{\chi}\tilde{\chi}}$  is smaller than  $b_{\tilde{\chi}\tilde{\chi}}$ , its contribution to  $\hat{\sigma}_{\text{eff}}$  in Eq. (21) is of the same order of magnitude as the one of  $b_{\tilde{\chi}\tilde{\chi}}$  which enters in this equation divided by a relative factor  $\lesssim x_F/3 \sim 8-9$ .

(ii) The main contribution to  $b_{\tilde{\chi}\tilde{\chi}}$  arises from the first term in the bracket in the right hand side of Eq. (24). The second term in this bracket is due to  $\tilde{\tau}_L\tilde{\tau}_R$  mixing.

(iii) The last term in the right hand side of Eq. (24) represents the contribution of the two lighter generations. Their right handed sleptons are considered degenerate with mass  $m_{\tilde{e}_R}$ . The off-diagonal elements in the slepton mass-squared matrices of the lighter families are negligible. The values of  $m_{\tilde{e}_R}$  are bigger than  $m_{\tilde{\tau}_2}$  and hence the corresponding contributions to  $b_{\tilde{\chi}\tilde{\chi}}$  are smaller than the ones from the  $\tilde{\tau}_2$  exchange. This is a major difference from models with low  $\tan\beta$ , where the contributions of all three diagrams with exchange of right handed sleptons are similar.

(iv) The contribution to  $b_{\tilde{\chi}\tilde{\chi}}$  of the diagram with a  $\tilde{\tau}_1$  exchange is small and, although taken into account in the computation, is not displayed in Eq. (24). We find that this contribution is suppressed by about  $1/6-1/8$  compared to the contribution of each of the lightest generations. This can be understood by the following observation. Despite the fact that the values of the mass in the propagator of this diagram,  $m_{\tilde{\tau}_1}$ , are not much higher than  $m_{\tilde{e}_R}$ , its main contribution contains a factor  $c_\theta^4 Y_L^4$ .

### B. Coannihilation cross sections

The contributions of the various coannihilation processes listed in Table I to the coefficients  $a_{ij}$  and  $b_{ij}$  ( $ij \neq \tilde{\chi}\tilde{\chi}$ ) in Eq. (19) are calculated using techniques similar to the ones in Ref. [32]. Leptons and quarks (except the  $t$  quark) in final states or propagators are taken to be massless. On the contrary, the  $b$  and  $\tau$  Yukawa couplings are not ignored since, in our case where  $\tan\beta$  is large, their influence turns out to be very significant. The most important contributions to  $\hat{\sigma}_{\text{eff}}$  in Eq. (21) arise from the  $a_{ij}$ 's in the case of coannihilation. In Table II, we list some of the processes contributing to the  $a_{ij}$ 's ( $ij \neq \tilde{\chi}\tilde{\chi}$ ) together with the analytical expressions for their contributions. In this table, a hat (or bar) over a quantity indicates that this quantity is measured in units of  $m_{\tilde{\tau}_2}$  (or  $m_{\tilde{\chi}} + m_{\tilde{\tau}_2}$ ) and the  $g$ 's will be defined shortly. Also,  $L_\tau = 1 - 2s_W^2$ ,  $R_\tau = -2s_W^2$  and

$$P_{1(2)} = 3\hat{m}_Z^4 - (+)4\hat{m}_Z^2 + 4, \quad P_3 = 3\hat{m}_Z^4 - 8\hat{m}_Z^2 + 8,$$

$$P_4 = 3\hat{m}_Z^6 - 3\hat{m}_Z^4 - 4\hat{m}_Z^2 + 4, \quad P_5 = 3\hat{m}_Z^4 - 5\hat{m}_Z^2 + 2. \quad (25)$$

The contribution of the process  $\tilde{\chi}\tilde{\tau}_2 \rightarrow \tau H$  (or  $\tau A$ ) to the coefficient  $a_{\tilde{\chi}\tilde{\tau}_2}$  is obtained from the expression for  $\tilde{\chi}\tilde{\tau}_2 \rightarrow \tau h$  in Table II by replacing  $h$  by  $H$  (or  $A$  and  $\cos 2\theta$  by 1).

TABLE II. Contributions to the coefficients  $a_{ij}$  ( $ij \neq \tilde{\chi}\tilde{\chi}$ ).

Process	Contribution to the coefficient $a_{ij}$
$\tilde{\chi}\tilde{\tau}_2 \rightarrow \tau h$	$e^2(1-\bar{m}_h^2)^2\{2Y_L Y_R g_{h\tau\tau}[2s_\theta c_\theta g_h/(m_{\tilde{\tau}_2}-\bar{m}_h^2 m_{\tilde{\chi}})-\cos 2\theta \bar{g}_{h1}/(\bar{m}_{\tilde{\tau}_1}^2+\bar{m}_{\tilde{\chi}}(\bar{m}_{\tilde{\tau}_2}-\bar{m}_h^2))]$ + $[g_{h\tau\tau}^2+g_\theta^2/(m_{\tilde{\chi}}\bar{m}_h^2-m_{\tilde{\tau}_2}^2)](s_\theta^2 Y_L^2+c_\theta^2 Y_R^2)+\bar{g}_{h1}^2(c_\theta^2 Y_L^2+s_\theta^2 Y_R^2)/(\bar{m}_{\tilde{\tau}_1}^2+\bar{m}_{\tilde{\chi}}(\bar{m}_{\tilde{\tau}_2}-\bar{m}_h^2))^2$ - $2s_\theta c_\theta(Y_L^2-Y_R^2)\bar{g}_h \bar{g}_{h1}/(\bar{m}_{\tilde{\tau}_2}-\bar{m}_{\tilde{\chi}}\bar{m}_h^2)(\bar{m}_{\tilde{\tau}_1}^2+\bar{m}_{\tilde{\chi}}(\bar{m}_{\tilde{\tau}_2}-\bar{m}_h^2))\}/32\pi c_W^2 m_{\tilde{\tau}_2}(m_{\tilde{\tau}_2}+m_{\tilde{\chi}})$
$\tilde{\chi}\tilde{\tau}_2 \rightarrow \tau\gamma$	$e^4(s_\theta^2 Y_L^2+c_\theta^2 Y_R^2)/16\pi c_W^2 m_{\tilde{\tau}_2}(m_{\tilde{\chi}}+m_{\tilde{\tau}_2})$
$\tilde{\chi}\tilde{\tau}_2 \rightarrow \tau Z$	$e^2(1-\bar{m}_Z^2)\{\bar{m}_{\tilde{\tau}_2}(1-\bar{m}_Z^2)^3[g_{\tilde{\tau}_1\tilde{\tau}_2Z}^2(s_\theta^2 Y_L^2+c_\theta^2 Y_R^2)/(\bar{m}_Z^2\bar{m}_{\tilde{\chi}}-\bar{m}_{\tilde{\tau}_2}^2)^2$ + $g_{\tilde{\tau}_1\tilde{\tau}_2Z}^2(c_\theta^2 Y_L^2+s_\theta^2 Y_R^2)/(\bar{m}_{\tilde{\tau}_1}^2+\bar{m}_{\tilde{\chi}}(\bar{m}_{\tilde{\tau}_2}-\bar{m}_Z^2))^2$ - $2g_{\tilde{\tau}_1\tilde{\tau}_2Z}g_{\tilde{\tau}_2\tilde{\tau}_2Z}s_\theta c_\theta(Y_L^2-Y_R^2)/(\bar{m}_{\tilde{\tau}_2}-\bar{m}_Z^2\bar{m}_{\tilde{\chi}})(\bar{m}_{\tilde{\tau}_1}^2+\bar{m}_{\tilde{\chi}}(\bar{m}_{\tilde{\tau}_2}-\bar{m}_Z^2))$ - $2g_Z(\bar{m}_Z^2-1)^2[g_{\tilde{\tau}_2\tilde{\tau}_2Z}(L_\tau s_\theta^2 Y_L^2+R_\tau c_\theta^2 Y_R^2)/(\bar{m}_{\tilde{\tau}_2}-\bar{m}_Z^2\bar{m}_{\tilde{\chi}})$ - $g_{\tilde{\tau}_1\tilde{\tau}_2Z}s_\theta c_\theta(L_\tau Y_L^2-R_\tau Y_R^2)/(\bar{m}_{\tilde{\tau}_1}^2+\bar{m}_{\tilde{\chi}}(\bar{m}_{\tilde{\tau}_2}-\bar{m}_Z^2))]$ + $g_Z^2(L_\tau s_\theta^2 Y_L^2+R_\tau c_\theta^2 Y_R^2)(1+\bar{m}_Z^2-2\bar{m}_Z^4)(1+\hat{m}_{\tilde{\chi}})\}/32\pi c_W^2 m_Z^2$
$\tilde{\tau}_2\tilde{\tau}_2 \rightarrow \tau\tau$	$e^4(s_\theta^4 Y_L^4+c_\theta^4 Y_R^4)m_{\tilde{\chi}}^2/\pi c_W^4 \Sigma_2^2$
$\tilde{\tau}_2\tilde{\tau}_2^* \rightarrow \gamma\gamma$	$e^4/8\pi m_{\tilde{\tau}_2}^2$
$\tilde{\tau}_2\tilde{\tau}_2^* \rightarrow \gamma Z$	$-e^2 g_{\tilde{\tau}_2\tilde{\tau}_2Z}^2(\hat{m}_Z^2-4)/16\pi m_{\tilde{\tau}_2}^2$
$\tilde{\tau}_2\tilde{\tau}_2^* \rightarrow ZZ$	$(1-\hat{m}_Z^2)^{1/2}\{[(g_h^2 g_{hZZ}^2 P_1/(\hat{m}_h^2-4)+12g_h g_{hZZ} g_{\tilde{\tau}_2\tilde{\tau}_2Z}^2 m_Z^2 \hat{m}_Z^2)/(\hat{m}_h^2-4)$ - $4g_h g_{hZZ} g_{\tilde{\tau}_1\tilde{\tau}_2Z}^2 m_{\tilde{\tau}_2}^2 (P_4-\hat{m}_{\tilde{\tau}_1}^2 P_1)/(1+\hat{m}_{\tilde{\tau}_1}^2-\hat{m}_Z^2)(\hat{m}_h^2-4)+(h \leftrightarrow H)]$ + $g_{\tilde{\tau}_2\tilde{\tau}_2Z}^4 m_Z^4 P_3/(\hat{m}_Z^2-2)^2+2g_h g_{hZZ} g_{HZZ} P_1/(\hat{m}_h^2-4)(\hat{m}_H^2-4)$ - $8g_{\tilde{\tau}_2\tilde{\tau}_2Z}^2 g_{\tilde{\tau}_1\tilde{\tau}_2Z}^2 m_Z^4 [P_5-3\hat{m}_{\tilde{\tau}_1}^2(\hat{m}_Z^2-2)]/(1+\hat{m}_{\tilde{\tau}_1}^2-\hat{m}_Z^2)(\hat{m}_Z^2-2)$ + $4m_{\tilde{\tau}_2}^4 g_{\tilde{\tau}_1\tilde{\tau}_2Z}^4 [\hat{m}_{\tilde{\tau}_1}^4 P_1+(1-\hat{m}_Z^2)^2 P_2-2\hat{m}_{\tilde{\tau}_1}^2 P_4]/(1+\hat{m}_{\tilde{\tau}_1}^2-\hat{m}_Z^2)^2\}/64\pi m_Z^4 m_{\tilde{\tau}_2}^2$ ( $1-\hat{m}_W^2$ ) $^{1/2}(4-4\hat{m}_W^2+3\hat{m}_W^4)[g_h g_{hW^+W^-}/(\hat{m}_h^2-4)$ + $g_{H} g_{HW^+W^-}/(\hat{m}_H^2-4)+g_{\tilde{\tau}_2\tilde{\tau}_2W^+W^-}^2/32\pi m_W^4 m_{\tilde{\tau}_2}^2$
$\tilde{\tau}_2\tilde{\tau}_2^* \rightarrow W^+W^-$	$3(1-\hat{m}_t^2)^{3/2}[g_h g_{htt}/(\hat{m}_h^2-4)+g_{H} g_{Htt}/(\hat{m}_H^2-4)]^2/4\pi m_{\tilde{\tau}_2}^4$
$\tilde{\tau}_2\tilde{\tau}_2^* \rightarrow t\bar{t}$	

For the contribution to  $a_{\tilde{\tau}_2\tilde{\tau}_2^*}$  of each of the five processes with two Higgs bosons in the final state (see Table I), a general formula can be given:

$$a_{\tilde{\tau}_2\tilde{\tau}_2^* \rightarrow H_p H_q} = \left( \frac{1}{2} \right) \frac{1}{128\pi m_{\tilde{\tau}_2}^6} [4 - (\hat{m}_{H_p} - \hat{m}_{H_q})^2]^{1/2} \times [4 - (\hat{m}_{H_p} + \hat{m}_{H_q})^2]^{1/2} \left( \frac{\lambda_h}{4 - \hat{m}_h^2} + \frac{\lambda_H}{4 - \hat{m}_H^2} \right. \\ \left. + \frac{4\lambda_1}{\hat{m}_{H_p}^2 + \hat{m}_{H_q}^2 - 2\hat{m}_{\tilde{\tau}_1}^2 - 2} \right. \\ \left. + \frac{4\lambda_2}{\hat{m}_{H_p}^2 + \hat{m}_{H_q}^2 - 4} - \lambda_c m_{\tilde{\tau}_2}^2 \right)^2, \quad (26)$$

where the  $H_p, H_q$  stand for  $h, H, A, H^+, H^-$ , the factor 1/2 enters only for identical particles in the final state and

$\lambda_h, \lambda_H, \lambda_1, \lambda_2, \lambda_c$  correspond to the diagrams  $s(h), s(H), t(\tilde{\tau}_{1,2})$  [or  $u(\tilde{\tau}_{1,2})$ ],  $c$  in Table I and are shown in the Table III.

The  $g$ 's in Tables II and III correspond to vertices with the particles entering indicated as subscripts. The simplest ones are (for Feynman rules, see, e.g., Ref. [33] with  $\mu \rightarrow -\mu$ )

$$g_{\tilde{\tau}_1\tilde{\tau}_2Z} = g_Z(-s_\theta c_\theta), \quad g_{\tilde{\tau}_2\tilde{\tau}_2Z} = g_Z(s_\theta^2 - 2s_W^2), \\ g_{\tilde{\tau}_2\tilde{\tau}_2W^+W^-} = g^2 s_\theta^2/2, \quad (27)$$

where  $g_Z = g/2c_W$  with  $g$  being the  $SU(2)_L$  gauge coupling constant. Note that  $g_A \equiv g_{\tilde{\tau}_2\tilde{\tau}_2A} = 0$ . The more complicated  $g$ 's are arranged in the Table IV, where we have defined

$$\tan 2\alpha = \tan 2\beta(m_A^2 + m_Z^2)/(m_A^2 - m_Z^2), \quad -\pi/2 \leq \alpha \leq 0. \quad (28)$$

TABLE III. The  $\lambda$  symbols.

Process	$\lambda_h$	$\lambda_H$	$\lambda_1$	$\lambda_2$	$\lambda_c$
$\tilde{\tau}_2 \tilde{\tau}_2^* \rightarrow hh$	$g_h g_{hh}$	$g_H g_{hH}$	$g_{h1}^2$	$g_h^2$	$g_{\tilde{\tau}_2 \tilde{\tau}_2}^2 hh$
$\tilde{\tau}_2 \tilde{\tau}_2^* \rightarrow hH$	$g_h g_{hH}$	$g_H g_{hH}$	$g_{h1} g_{H1}$	$g_h g_H$	$g_{\tilde{\tau}_2 \tilde{\tau}_2}^2 hH$
$\tilde{\tau}_2 \tilde{\tau}_2^* \rightarrow HH$	$g_h g_{hH}$	$g_H g_{HH}$	$g_{H1}^2$	$g_H^2$	$g_{\tilde{\tau}_2 \tilde{\tau}_2}^2 HH$
$\tilde{\tau}_2 \tilde{\tau}_2^* \rightarrow AA$	$g_h g_{AA}$	$g_H g_{AA}$	$-g_{A1}^2$	0	$g_{\tilde{\tau}_2 \tilde{\tau}_2}^2 AA$
$\tilde{\tau}_2 \tilde{\tau}_2^* \rightarrow H^+ H^-$	$g_h g_{H^+ H^-}$	$g_H g_{H^+ H^-}$	0	0	$g_{\tilde{\tau}_2 \tilde{\tau}_2}^2 H^+ H^-$

We do not show explicitly the small contributions to  $a_{\tilde{\tau}_2 \tilde{\tau}_2^*}$  of the processes with  $b\bar{b}$  and  $\tau\bar{\tau}$  in the final state. They are, however, taken into account in the computation. The contributions to  $a_{\tilde{\tau}_2 \tilde{\tau}_2^*}$  of the processes with  $u\bar{u}$ ,  $d\bar{d}$  and  $e\bar{e}$  in the final state vanish (these processes contribute only to  $b$ 's). Also, the coefficients  $b_{ij}$  ( $ij \neq \tilde{\chi}\tilde{\chi}$ ), although included in the calculation, are not displayed since their contribution to  $\hat{\sigma}_{\text{eff}}$  is, in general, negligible. Note that many of the couplings and terms listed above have not been included in previous calculations [14] with small  $\tan \beta$ . Some comments are now in order.

(i) All five processes for the coannihilation of  $\tilde{\chi}$  with  $\tilde{\tau}_2$  listed in Table I give more or less comparable contributions to the coefficient  $a_{\tilde{\chi}\tilde{\tau}_2}$  (the leading contribution comes, in general, from  $\tilde{\chi}\tilde{\tau}_2 \rightarrow \tau h$ ). The relative contribution of  $b_{\tilde{\chi}\tilde{\tau}_2}$  to  $\hat{\sigma}_{(\tilde{\chi}\tilde{\tau}_2)}$  in Eq. (21) turns out to be essentially independent of  $m_A$  ( $95 \text{ GeV} \leq m_A \leq 220 \text{ GeV}$ ). This contribution varies from about 5 to about 8 % as  $\Delta_{\tilde{\tau}_2}$  increases from 0 to 0.1 (this is the relevant range of  $\Delta_{\tilde{\tau}_2}$  as we shall see).

(ii) The major contributions to  $a_{\tilde{\tau}_2 \tilde{\tau}_2^*}$  come from the processes  $\tilde{\tau}_2 \tilde{\tau}_2^* \rightarrow hh, t\bar{t}$ , and  $\tilde{\tau}_2 \tilde{\tau}_2 \rightarrow \tau\tau$ . However, many of the other relevant processes in Table I (such as  $\tilde{\tau}_2 \tilde{\tau}_2^* \rightarrow ZZ, \gamma\gamma, HH, AA, H^+ H^-$ ,  $\gamma Z$ ) have, in general, important contributions which cannot be neglected ( $\tilde{\tau}_2 \tilde{\tau}_2^* \rightarrow ZZ$ , for large  $\Delta_{\tilde{\tau}_2}$ 's and  $m_A$ 's, gives a major contribution). Also, the reaction  $\tilde{\tau}_2 \tilde{\tau}_2^* \rightarrow hH(W^+ W^-)$  is enhanced for low values of  $m_A$  (and  $\Delta_{\tilde{\tau}_2}$ ). The relative contribution of  $b_{\tilde{\tau}_2 \tilde{\tau}_2^*}$  to  $\hat{\sigma}_{(\tilde{\tau}_2 \tilde{\tau}_2^*)}$ , which can be either positive or negative, is less than about 1 % for all relevant values of parameters.

(iii) For  $\Delta_{\tilde{\tau}_2} = 0$ , the contribution of the  $\tilde{\chi}$  annihilation to  $\hat{\sigma}_{\text{eff}}$  is very small ( $\approx 0.4\%$ ). The corresponding contributions of  $\hat{\sigma}_{(\tilde{\chi}\tilde{\tau}_2)}$  and  $\hat{\sigma}_{(\tilde{\tau}_2 \tilde{\tau}_2^*)}$  span the ranges 27–24 % and 73–76 %, respectively, as  $m_A$  varies from 95 to 220 GeV. For  $\Delta_{\tilde{\tau}_2} = 0.1$ , however, the annihilation of  $\tilde{\chi}$ 's becomes very significant accounting for about 33–31 % of  $\hat{\sigma}_{\text{eff}}$ . The most important contribution ( $\approx 58\%$  of  $\hat{\sigma}_{\text{eff}}$ ), in this case, comes

TABLE IV.  $g$  symbols.

$g$ symbol	Expression
$g_{h[H]1}$ ( $\equiv g_{\tilde{\tau}_1 \tilde{\tau}_2 h[H]}$ )	$g_Z m_Z \sin[-\cos](\alpha + \beta)(L_\tau + R_\tau) s_\theta c_\theta \\ + g m_\tau \cos 2\theta (A_\tau \sin[-\cos]\alpha - \mu \cos[\sin]\alpha) / 2m_W \cos \beta \\ - g_Z m_Z \sin[-\cos](\alpha + \beta)(L_\tau s_\theta^2 - R_\tau c_\theta^2) - (g m_\tau / m_W \cos \beta) \\ \{-m_\tau \sin[-\cos]\alpha - s_\theta c_\theta (A_\tau \sin[-\cos]\alpha - \mu \cos[\sin]\alpha)\}$
$g_{h[H]}$ ( $\equiv g_{\tilde{\tau}_2 \tilde{\tau}_2 h[H]}$ )	$g m_\tau (A_\tau \tan \beta - \mu) / 2m_W \\ - [+] g_Z^2 \cos 2\alpha (L_\tau s_\theta^2 - R_\tau c_\theta^2) - g^2 (\sin[\cos]\alpha / \cos \beta)^2 m_\tau^2 / 2m_W^2 \\ g^2 \sin 2\alpha (-L_\tau / 2c_W^2 + m_\tau^2 / 2m_W^2 \cos^2 \beta) s_\theta^2 / 2 \\ + g^2 \sin 2\alpha (-\tan^2 \theta_W + m_\tau^2 / 2m_W^2 \cos^2 \beta) c_\theta^2 / 2 \\ - g_Z^2 \cos 2\beta (L_\tau s_\theta^2 - R_\tau c_\theta^2) - g^2 \tan^2 \beta (m_\tau / m_W)^2 / 2 \\ g^2 \cos 2\beta (1 - L_\tau / 2c_W^2) s_\theta^2 - \tan^2 \theta_W c_\theta^2 / 2 \\ - g^2 \tan^2 \beta (m_\tau / m_W)^2 c_\theta^2 / 2 \\ - 3 g_Z m_Z \sin[\cos](\alpha + \beta) \cos 2\alpha$
$g_{A1}$ ( $\equiv g_{\tilde{\tau}_1 \tilde{\tau}_2 A}$ )	$g_Z m_Z \sin[\cos](\alpha + \beta) \cos 2\alpha \\ - g_Z m_Z \sin[-\cos](\alpha + \beta) \cos 2\beta \\ - g \{m_W \sin[\cos](\beta - \alpha) + m_Z \sin[-\cos](\alpha + \beta) \cos 2\beta / 2c_W\}$
$g_{\tilde{\tau}_2 \tilde{\tau}_2 hh}$	$g m_Z \sin[\cos](\beta - \alpha) / c_W \\ g m_W \sin[\cos](\beta - \alpha)$
$g_{\tilde{\tau}_2 \tilde{\tau}_2 HH}$	$- g (\cos[\sin]\alpha / \sin \beta) (m_\tau / 2m_W) \\ g (\sin[-\cos]\alpha / \cos \beta) (m_\tau / 2m_W) \\ - g \tan \beta (m_\tau / 2m_W)$
$g_{\tilde{\tau}_2 \tilde{\tau}_2 AA}$	
$g_{\tilde{\tau}_2 \tilde{\tau}_2 H^+ H^-}$	
$g_{h[H]ZZ}$	
$g_{h[H]W^+ W^-}$	
$g_{h[H]tt}$	
$g_{h[H]\tau\tau}$	
$g_{A\tau\tau}$	

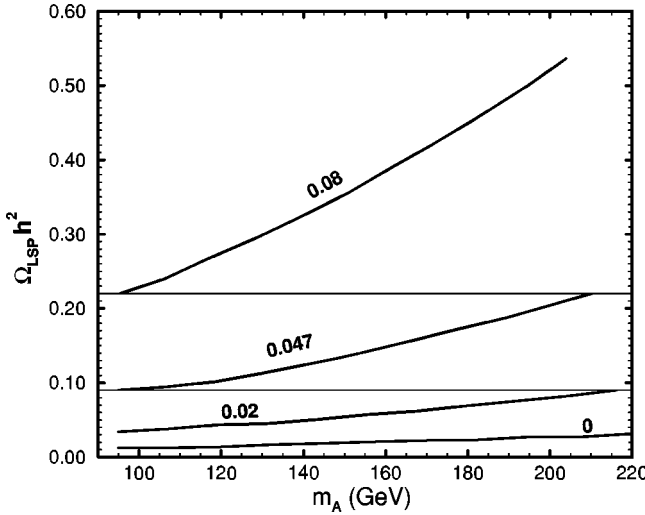


FIG. 3. The LSP abundance  $\Omega_{\text{LSP}} h^2$  as a function of  $m_A$  for  $\Delta_{\tilde{\tau}_2}=0, 0.02, 0.047$ , and  $0.08$  as indicated. The limiting lines at  $\Omega_{\text{LSP}} h^2=0.09$  and  $0.22$  are also included.

from the coannihilation of  $\tilde{\chi}$  with  $\tilde{\tau}_2$ , whereas  $\tilde{\tau}_2$  coannihilation with  $\tilde{\tau}_2$  or  $\tilde{\tau}_2^*$  accounts for about 9–11 % of  $\hat{\sigma}_{\text{eff}}$ . We see that, although  $\tilde{\chi}$  annihilation is negligible for small  $\Delta_{\tilde{\tau}_2}$ 's, it is strongly enhanced at higher values of  $\Delta_{\tilde{\tau}_2}$ . This is due to the fact that the abundance of  $\tilde{\tau}_2$ 's decreases relative to the one of  $\tilde{\chi}$ 's as  $\Delta_{\tilde{\tau}_2}$  increases.

(iv) For  $\Delta_{\tilde{\tau}_2}=0$ , the contributions of  $b_{\tilde{\chi}\tilde{\tau}_2}$  and  $b_{\tilde{\tau}_2\tilde{\tau}_2^{(*)}}$  to  $\hat{\sigma}_{\text{eff}}$  cancel each other partially and, thus, an accurate result (error  $\approx 0.5\%$ ) can be obtained by ignoring these  $b$ 's. For  $\Delta_{\tilde{\tau}_2}=0.1$ , however, the contribution of  $b_{\tilde{\chi}\tilde{\tau}_2}$  dominates strongly over the one of  $b_{\tilde{\tau}_2\tilde{\tau}_2^{(*)}}$  and gives  $\approx 4-5\%$  of  $\hat{\sigma}_{\text{eff}}$ . Consequently, our results can be reproduced with an accuracy better than  $\approx 5\%$  by using, for coannihilation, just the  $a$ 's. Their analytical expressions have been given earlier in this section. On the contrary, the  $b_{\tilde{\chi}\tilde{\chi}}$  cannot be ignored since its contribution to  $\hat{\sigma}_{(\tilde{\chi}\tilde{\chi})}$  can be as high as 80% and the annihilation of  $\tilde{\chi}$ 's is very significant at higher  $\Delta_{\tilde{\tau}_2}$ 's.

### C. Results on $\Omega_{\text{LSP}} h^2$

We can now proceed to the evaluation of  $\Omega_{\text{LSP}} h^2$ . The top quark mass  $m_t(m_t)$  is again fixed at 166 GeV. For given values of  $\Delta_{\tilde{\tau}_2}$  and  $m_A$ , all the particle physics parameters of the model are determined (see Sec. II). The freeze-out parameter  $x_F$  can then be found by solving Eq. (18) and  $\hat{\sigma}_{\text{eff}}$  is evaluated from Eq. (21). The LSP relic abundance  $\Omega_{\tilde{\chi}} h^2$  is estimated using Eq. (16) and is depicted in Fig. 3 as function of  $m_A$  for  $\Delta_{\tilde{\tau}_2}=0, 0.02, 0.047$ , and  $0.08$ . Remember that the curves on this plot, which correspond to specific values of  $\Delta_{\tilde{\tau}_2}$ , terminate at the appropriate upper limit on  $m_A$  (derived from the restriction  $M_{1/2} \leq 800$  GeV). This limit decreases as  $\Delta_{\tilde{\tau}_2}$  increases.

Requiring  $\Omega_{\tilde{\chi}} h^2$  to be confined in the cosmologically allowed range 0.09–0.22, one finds that  $\Delta_{\tilde{\tau}_2}$  is restricted be-

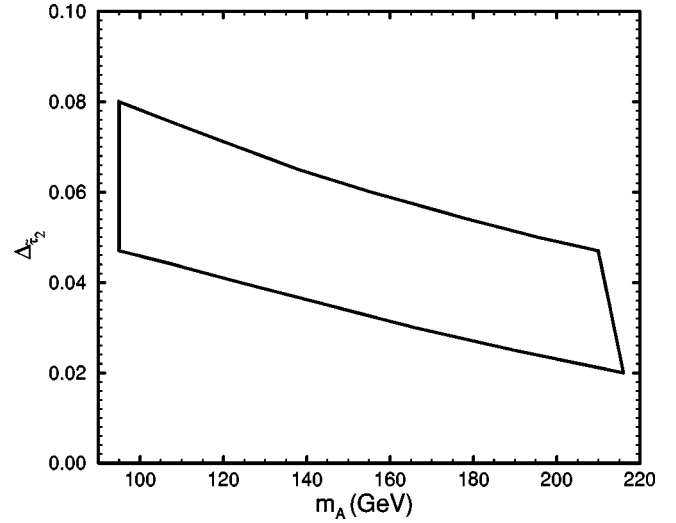


FIG. 4. The cosmologically allowed region in the  $m_A - \Delta_{\tilde{\tau}_2}$  plane, where  $\Omega_{\text{LSP}} h^2$  lies in the range  $0.09-0.22$ . We also take  $m_A \geq 95$  GeV and  $M_{1/2} \leq 800$  GeV.

tween  $\approx 0.02$  and  $0.08$ . Note that the upper limit on  $\Delta_{\tilde{\tau}_2}$  does not depend on our restriction on  $M_{1/2}$ . On the contrary, the lower limit on  $\Delta_{\tilde{\tau}_2}$  is somewhat dependent on the particular choice one makes for this restriction. This deserves further study which would require going beyond the simplifying assumption of a common supersymmetry threshold  $M_S$ . It should be pointed out that this lower bound on  $\Delta_{\tilde{\tau}_2}$  is anyway evaded if there exist additional contributions to the cold dark matter of the universe from particle species other than  $\tilde{\chi}$ .

Figure 4 shows the cosmologically allowed region in the  $m_A - \Delta_{\tilde{\tau}_2}$  plane obtained from the above considerations. We see that  $m_A$  can vary only between about 95 and 216 GeV.

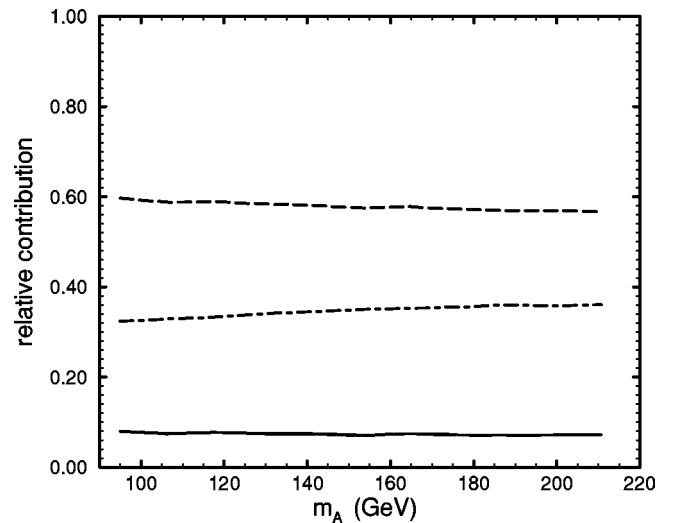


FIG. 5. The relative contributions  $\hat{\sigma}_{(\tilde{\chi}\tilde{\chi})}/\hat{\sigma}_{\text{eff}}$  (solid line),  $\hat{\sigma}_{(\tilde{\tau}_2\tilde{\tau}_2)}/\hat{\sigma}_{\text{eff}}$  (dashed line), and  $\hat{\sigma}_{(\tilde{\tau}_2\tilde{\tau}_2^*)}/\hat{\sigma}_{\text{eff}}$  (dot-dashed line) of the three inclusive (co)annihilation reactions to  $\hat{\sigma}_{\text{eff}}$  as functions of  $m_A$  for  $\Delta_{\tilde{\tau}_2}=0.047$ .

The lower (upper) boundary of this region corresponds to  $\Omega_{\tilde{\chi}} h^2 = 0.09$  (0.22). The left boundary corresponds to  $M_{1/2} = 800$  GeV ( $0.09 \leq \Omega_{\tilde{\chi}} h^2 \leq 0.22$ ). Along this line,  $m_{\tilde{\chi}}$  is essentially constant and acquires its maximal allowed value  $\approx 354$  GeV (see Fig. 2). The minimal value of the LSP mass is obtained at the lower left corner of this allowed region, where  $\Delta_{\tilde{\tau}_2} \approx 0.047$ , and is equal to about 222 GeV (see Fig. 2). We, thus, see that the LSP mass ranges between  $\approx 222$  and 354 GeV. The  $\tilde{\tau}_2$  mass is bounded between about 232 and 369 GeV which makes  $\tilde{\tau}_2$  a phenomenologically interesting charged sparticle. The upper (lower) bound corresponds to the upper right (lower left) corner of the region in Fig. 4. Actually, the whole sparticle mass spectrum is strongly restricted by our considerations. Note, however, that the upper bounds on the sparticle masses depend on our choice for the maximal allowed  $M_{1/2}$ . This requires a detailed study with inclusion of one-loop and supersymmetry threshold effects which may not be negligible for higher  $M_{1/2}$ 's.

The relative contributions  $\hat{\sigma}_{(ij)}/\hat{\sigma}_{\text{eff}} [(ij) = (\tilde{\chi}\tilde{\chi}), (\tilde{\chi}\tilde{\tau}_2), (\tilde{\tau}_2\tilde{\tau}_2^{(*)})]$  of the three inclusive (co)annihilation reactions to  $\hat{\sigma}_{\text{eff}}$  are given in Fig. 5 as functions of  $m_A$  for the “central” value of  $\Delta_{\tilde{\tau}_2} = 0.047$ . The allowed range of  $m_A$  is 95–211 GeV in this case.

#### IV. CONCLUSIONS

We considered the MSSM with gauge and Yukawa coupling unification employing radiative electroweak symmetry breaking with universal boundary conditions from gravity-mediated supersymmetry breaking. We calculated the relic density of the LSP (an almost pure  $B$ -ino). Coannihilation of the LSP with the NLSP (the lightest stau) is crucial for reducing its relic density to an acceptable level. Compatibility with the mixed or the pure cold (with a nonzero cosmological constant) dark matter scenarios for structure formation in the universe requires that the lightest stau mass is about 2–8 % larger than the  $B$ -ino mass. This combined with the fact that the LSP mass is restricted to be greater than about 222 GeV allows the lightest stau mass to be as low as 232 GeV.

#### ACKNOWLEDGMENTS

We thank B. Ananthanarayan, C. Boehm, M. Drees, N. Fornengo, S. Khalil, A. B. Lahanas, K. Olive, and N. D. Vlachos for discussions. One of us (C.P.) thanks P. Porfyriadis for computational help and the Greek State Scholarship Institution (I.K.Y) for support. This work was supported by the European Union under TMR Contract No. ERBFMRX-CT96-0090 and the Greek Government research Grant No. PENED/95 K.A.1795.

---

[1] E. Gawiser and J. Silk, *Science* **280**, 1405 (1998).  
 [2] Q. Shafi and F. W. Stecker, *Phys. Rev. Lett.* **53**, 1292 (1984); for a recent review and other references see Q. Shafi and R. K. Schaefer, hep-ph/9612478.  
 [3] T. Kajita, talk given at the XVIIIth International Conference on Neutrino Physics and Astrophysics (Neutrino '98), Takayama, Japan, 1998.  
 [4] G. Lazarides, *Phys. Lett. B* **452**, 227 (1999).  
 [5] A. E. Evrard, *Mon. Not. R. Astron. Soc.* **292**, 289 (1997).  
 [6] S. Burles and D. Tytler, *Astrophys. J.* **499**, 699 (1998); **507**, 732 (1998).  
 [7] B. Schmidt *et al.*, *Astrophys. J.* **507**, 46 (1998); A. Riess *et al.*, *Astron. J.* **116**, 1009 (1998); S. Perlmutter *et al.*, *Bull. Am. Astron. Soc.* **29**, 1351 (1997).  
 [8] L. Krauss and M. S. Turner, *Gen. Relativ. Gravit.* **27**, 1137 (1995); J. P. Ostriker and P. J. Steinhardt, *Nature* (London) **377**, 600 (1995); A. R. Liddle *et al.*, *Mon. Not. R. Astron. Soc.* **282**, 281 (1996).  
 [9] J. R. Primack and M. A. K. Gross, astro-ph/9810204.  
 [10] G. Lazarides and N. D. Vlachos, *Phys. Lett. B* **459**, 482 (1999).  
 [11] H. Goldberg, *Phys. Rev. Lett.* **50**, 1419 (1983).  
 [12] J. Ellis, J. S. Hagelin, D. V. Nanopoulos, K. A. Olive, and M. Srednicki, *Nucl. Phys.* **B238**, 453 (1984).  
 [13] M. Drees and M. M. Nojiri, *Phys. Rev. D* **47**, 376 (1993); M. Drees, hep-ph/9703260.  
 [14] J. Ellis, T. Falk, and K. A. Olive, *Phys. Lett. B* **444**, 367 (1998); J. Ellis, T. Falk, G. Ganis, K. A. Olive, and M. Schmitt, *Phys. Rev. D* **58**, 095002 (1998); J. Ellis, T. Falk, K. A. Olive, and M. Srednicki, hep-ph/9905481.  
 [15] A. B. Lahanas, D. V. Nanopoulos, and V. C. Spanos, *Phys. Lett. B* **464**, 213 (1999).  
 [16] K. Griest and D. Seckel, *Phys. Rev. D* **43**, 3191 (1991).  
 [17] S. Mizuta and M. Yamaguchi, *Phys. Lett. B* **298**, 120 (1993); P. Gondolo and J. Edsjo, *Phys. Rev. D* **56**, 1879 (1997).  
 [18] B. Ananthanarayan, G. Lazarides, and Q. Shafi, *Phys. Rev. D* **44**, 1613 (1991). For a more recent update see U. Sarid, hep-ph/9610341.  
 [19] B. Ananthanarayan, G. Lazarides, and Q. Shafi, *Phys. Lett. B* **300**, 245 (1993); L. J. Hall, R. Rattazzi, and U. Sarid, *Phys. Rev. D* **50**, 7048 (1994); V. Barger, M. S. Berger, and P. Ohmann, *ibid.* **47**, 1093 (1993); P. Langacker and N. Polonsky, *ibid.* **49**, 1454 (1994).  
 [20] M. Carena, M. Olechowski, S. Pokorski, and C. E. M. Wagner, *Nucl. Phys.* **B426**, 269 (1994).  
 [21] B. Ananthanarayan, Q. Shafi, and X. M. Wang, *Phys. Rev. D* **50**, 5980 (1994).  
 [22] V. Barger, M. S. Berger, and P. Ohmann, *Phys. Rev. D* **49**, 4908 (1994); M. Drees and M. M. Nojiri, *Nucl. Phys.* **B369**, 54 (1992); M. Olechowski and S. Pokorski, *ibid.* **B404**, 590 (1993).  
 [23] G. Gamberini, G. Ridolfi, and F. Zwirner, *Nucl. Phys.* **B331**, 331 (1990).  
 [24] D. M. Pierce, J. A. Bagger, K. T. Matchev, and R. Zhang, *Nucl. Phys.* **B491**, 3 (1997).  
 [25] H. Baer, M. Brhlik, D. Castaño, and X. Tata, *Phys. Rev. D* **58**, 015007 (1998).  
 [26] This problem arises in the simplest realization of the SO(10)

model with universal boundary conditions and Yukawa coupling unification, where the electroweak Higgs bosons exclusively belong to a SO(10) 10-plet. However, in a complete SO(10) model of this variety, which correctly incorporates fermion masses and mixings, the electroweak Higgs bosons will receive smaller contributions from other representations too. Under some circumstances [see, e.g., G. Lazarides and Q. Shafi, Nucl. Phys. **B350**, 179 (1991)], these contributions can affect only the down quark and lepton masses leaving, in particular, the top quark mass unaltered. The details of the scheme can then be arranged so that  $m_b(m_Z)$  becomes experimentally acceptable, while  $m_\tau$  and  $\tan \beta$  are minimally affected. Alternatively, small GUT threshold corrections to gauge (or Yukawa) coupling unification can also help to reduce  $m_b$  in specific models without abandoning universal boundary conditions. An example with a small negative GUT correction to  $\alpha_s$  and acceptable value of  $m_b$  can be found in T. Blažek and S. Raby, Phys. Rev. D **59**, 095002 (1999). It is interesting that

such a correction to  $\alpha_s$  is anyway needed for gauge coupling unification [24]. Our LSP relic density calculation is not affected in any essential way by these modifications of the simplest scheme.

- [27] H. Baer, C. Chen, M. Drees, F. Paige, and X. Tata, Phys. Rev. Lett. **79**, 986 (1997).
- [28] M. Drees and M. M. Nojiri, Phys. Rev. D **45**, 2482 (1992).
- [29] J. Ellis, G. Ridolfi, and F. Zwirner, Phys. Lett. B **262**, 477 (1991).
- [30] E. W. Kolb and M. S. Turner, *The Early Universe* (Addison-Wesley, Redwood City, CA, 1990).
- [31] K. Griest, M. Kamionkowski, and M. S. Turner, Phys. Rev. D **41**, 3565 (1990).
- [32] L. Roszkowski, Phys. Rev. D **50**, 4842 (1994); J. Wells, hep-ph/9404219.
- [33] H. Haber and G. L. Kane, Phys. Rep. **117**, 75 (1985); J. Gunion and H. Haber, Nucl. Phys. **B272**, 1 (1986); **B402**, 567(E) (1993).